



# Chelation of heavy group 2 (radio)metals by *p*-tert-butylcalix[4]arene-1,3-crown-6 and logK determination via NMR

David Bauer<sup>a,b</sup>, Matthew Gott<sup>a</sup>, Jörg Steinbach<sup>a,b</sup>, Constantin Mamat<sup>a,b,\*</sup>

<sup>a</sup> Helmholtz-Zentrum Dresden-Rossendorf, Institut für Radiopharmazeutische Krebsforschung, Bautzner Landstraße 400, D-01328 Dresden, Germany

<sup>b</sup> Technische Universität Dresden, Fakultät Chemie und Lebensmittelchemie, D-01062 Dresden, Germany

## ARTICLE INFO

### Article history:

Received 12 December 2017

Received in revised form 9 February 2018

Accepted 12 March 2018

Available online 13 March 2018

### Keywords:

Calix[4]crown complex

Barium

Stability constant

<sup>207</sup>Pb NMR

Radium

## ABSTRACT

A crown-bridged calix[4]arene scaffold was investigated as lead compound for the ligation of heavy alkaline earth metals such as strontium and barium, which appear to be useful for radiopharmaceutical applications in diagnosis as well as in radiotherapy. In particular barium, due to its chemical similarities, could serve as a surrogate for radium, a metal of high radiopharmaceutical interest. The ability of *p*-tert-butylcalix[4]arene-1,3-crown-6 (**1**) in particular to chelate cations, such as group 1 and 2 metal ions or ammonium ions is well known. Also, the manifold possibilities of structural modification on the upper- and lower-rim as well as on the crown itself produce properties that may lead to a highly selective and effective chelating agent. In this work, titration experiments of the perchlorate salts of Ba<sup>2+</sup>, Sr<sup>2+</sup> and Pb<sup>2+</sup> with ligand **1** were performed to determine their stability constants (logK = 4.7, 4.3, and 3.3, respectively) by <sup>1</sup>H NMR measurements in acetonitrile-*d*<sub>3</sub>.

© 2018 Elsevier B.V. All rights reserved.

## 1. Introduction

Radium is the heaviest known member of the alkaline earth metals and all 33 of its isotopes are radioactive [1]. Four of these isotopes are available from the decay of primordial nuclides [2]. Two of these, radium-223 and radium-224, have suitable half-lives (<sup>223</sup>Ra: 11.4 d, <sup>224</sup>Ra: 3.6 d) and nuclear decay properties that make them useful tools for alpha particle therapy [3]. Alpha particles are highly energetic (5–9 MeV) and create frequent ionization events (approx. 80 keV/μm) across a short path length (40–100 μm), which leads to a high effectiveness for tumor cell killing [4]. Both <sup>223</sup>Ra and <sup>224</sup>Ra rapidly decay via series of six daughter nuclides (four alpha and two beta particles) to stable <sup>207</sup>Pb and <sup>208</sup>Pb, respectively, which results in massive energetic emissions of 28 and 27 MeV, respectively [1]. In 2013, [<sup>223</sup>Ra]RaCl<sub>2</sub> (Xofigo®) became the first and, until now, the only alpha-emitting radiopharmaceutical to receive FDA and EMEA approval for clinical use.

The homologous elements barium and strontium exist as stable nuclides, but offer radioisotopes for radiopharmaceutical applications [5]. <sup>131</sup>Ba (E<sub>γ</sub> = 496 keV, 48%) and <sup>135m</sup>Ba (E<sub>γ</sub> = 268 keV, 16%) are both possible γ-emitters for diagnostic use and were broadly discussed as bone-scanning agents in scintigraphy [6–8]. <sup>90</sup>Sr (E<sub>β,max</sub> = 546 keV, 100%) also finds extensive application as a strong beta-emitter for superficial brachytherapy of some cancers [7,9,10]. No literature was

found regarding the application of the light alkaline earth metals beryllium, magnesium, and calcium for therapy or diagnosis.

Searching for suitable ligands, a group of molecular baskets termed calix[4]arenes was found to be a promising start. Calix[4]arenes are metacyclophanes having a hydrophobic cavity between the lower and upper rim, formed by four *p*-tert-butylphenol units bridged with methylene links [11]. This class of macromolecules is known for a wide range of applications [12,13], most likely due to their numerous possibilities for functionalization [14]. Calix[4]arenes act as biologically active compounds and are used as antibacterial and even anti-malarial agents or in cancer chemotherapy [15–18]. Additionally, they can be promising enzyme inhibitors or interact with amino acids [19,20]. Their ability to form inclusion compounds with neutral molecules or ions makes them useful as sensors, catalysts, ligands or, when bound to a resin, as effective separation agents for ions [21–26].

The calix[4]arene framework can also be seen as a platform for building an optimized chelator. On the lower rim, there are four hydroxyl groups. Two can be functionalized as proton-ionizable groups to form a neutral complex with divalent cations; the remaining two can be bridged by a crown ether. With this concept, both the advantages of the electrostatic, macrocyclic, and cryptate effect are combined. Another benefit of the calix[4]crown-6 scaffold is the easy access [27,28]. To provide the ideal cavity for heavy group 2 metals, it is essential to choose a suitable crown size. The group around Bartsch focused on extraction of alkaline earth metal cations using calixcrowns [29–31]. As a result of their studies, calix[4]arene-1,3-crown-6 derivatives have been found very effective for Ba<sup>2+</sup>. Barium, strontium and radium possess analogous chemical properties and their radii are of a similar range

\* Corresponding author at: Helmholtz-Zentrum Dresden-Rossendorf, Institut für Radiopharmazeutische Krebsforschung, Bautzner Landstraße 400, D-01328 Dresden, Germany.

E-mail address: [c.mamat@hzdr.de](mailto:c.mamat@hzdr.de) (C. Mamat).

[32], therefore, these studies were considered to be a useful starting point. Additionally, these compounds showed a high selectivity for barium over the lighter alkaline earth metals or alkali metals, however,  $\text{Ra}^{2+}$  was not investigated. Van Leeuwen et al. [33–35] compared the efficiency of various ligands including calixarenes as ionophores for  $\text{Ra}^{2+}$  extraction in the case of nuclear waste management. They also investigated derivatives of *p*-tert-butylcalix[4]arene-1,3-crown-6 (**1**) and showed that they have high extraction rates and a suitable selectivity in contrast to simple (aza-)crown ethers. In radiopharmacy, a high stability constant of the complex is important so that a radium release and accumulation in bone tissue is minimized.

The objective of this research was to evaluate *p*-tert-butylcalix[4]arene-1,3-crown-6 (**1**) as a possible leading compound that could, upon further modification, yield a viable chelator for heavy group 2 metals in radiopharmaceutical application. Existing literature about group 2 metal ligands specifically with radium are focused mainly on extraction studies, while useful, this does not provide information about comparable stability constants [30,33,36]. Therefore, a reliable and constant method for the calculation of stability constants with barium and strontium via NMR spectroscopy was developed to determine the efficiency of ligand **1**. Since there is no stable radium isotope, barium is additionally used as non-radioactive surrogate, due to its related chemical behavior, *in vivo* distribution, and size [2,37,38]. To further guarantee the size selectivity of the basic structure, sodium and tetrabutylammonium cation were additionally investigated. Referring to radiopharmaceutical application, the competitors of interest are the ions, which primarily occur in blood plasma, such as sodium. This ion is normally found in high concentrations (135–150 mM) and is therefore of particular relevance [39].

Furthermore, the interaction of ligand **1** and  $\text{Pb}^{2+}$  was studied by using  $^1\text{H}$  and  $^{207}\text{Pb}$  NMR spectroscopy. For our research, lead is also a metal of interest. On the one hand, it is the stable end product of both radium decay chains. On the other hand,  $^{212}\text{Pb}$  is a promising  $\beta^-$ -emitter (570 keV max  $\beta^-$ , 12%), and a feasible candidate for radiopharmaceutical applications, since it can also be used as an *in vivo* generator for  $^{212}\text{Bi}$ , which is a strong alpha emitter [40,41].

## 2. Experimental Section

### 2.1. General

$^1\text{H}$  NMR spectra were recorded on an Agilent DD2–400 MHz NMR spectrometer with ProbeOne at 298 K. Chemical shifts of the spectra were reported in parts per million (ppm) using TMS as internal standard. All  $^{207}\text{Pb}$  spectra were recorded at a frequency of 125.1 MHz on an Agilent DD2–600 MHz NMR spectrometer with ProbeOne at 298 K using a  $90^\circ$  pulse width of 6.0  $\mu\text{s}$ , a 0.157 s acquisition time, and a 0.6 s delay time. A 1.0 M  $\text{Pb}(\text{NO}_3)_2$  solution (natural) was used as an external standard ( $\delta = -2965$  ppm,  $\text{D}_2\text{O}$ , 25  $^\circ\text{C}$ ; relative to  $\text{PbMe}_4$ ). For the synthesis of ligand **1**, 4-tert-butylcalix[4]arene (abcr, 99%), pentaethylene glycol di(*p*-toluenesulfonate) (Alfa Aesar, 95%), potassium carbonate anhydrous (Acros, 99 + %), acetonitrile (Fisher Scientific, HPLC-grade), dichloromethane (Fisher Scientific, HPLC-grade), hydrochloric acid (Merck, 37%), and sodium sulfate anhydrous (Alfa Aesar, 99%) were used as obtained. Preparative column chromatography was carried out with silica gel 60 (Merck, particle size 0.040–0.063 mm), petroleum ether (Fisher Scientific, bp 40–60  $^\circ\text{C}$ , analytical reagent grade), and ethyl acetate (Fisher Scientific, HPLC-grade). For the preparation of the complexes, barium perchlorate (Alfa Aesar, 99%), sodium perchlorate (Alfa Aesar, 98%), strontium perchlorate (abcr, 99.9%), and tetrabutylammonium perchlorate (Acros, 98%) were dried at room temperature under vacuum and used without further purification. Lead (II) perchlorate trihydrate (abcr, 97%) was used as obtained. The solvents used for NMR measurements were purchased from Deutero GmbH.

### 2.2. Synthesis of ligand **1**

*p*-tert-Butylcalix[4]arene-1,3-crown-6 (**1**) was synthesized according to the literature [29]. Briefly, a suspension of *p*-tert-butylcalix[4]arene (1.00 g, 1.54 mmol), pentaethylene glycol di(*p*-toluenesulfonate) (924 mg, 1.69 mmol) and  $\text{K}_2\text{CO}_3$  (256 mg, 1.85 mmol) in acetonitrile (100 mL) was refluxed under argon for 7 days. After cooling to rt, the solvent was removed and  $\text{CH}_2\text{Cl}_2$  (50 mL) was added. The suspension was washed with 10% HCl ( $2 \times 50$  mL) and water ( $1 \times 50$  mL). The organic layer was dried over  $\text{Na}_2\text{SO}_4$ . After evaporation of  $\text{CH}_2\text{Cl}_2$ , the crude mixture was purified by column chromatography ( $\text{SiO}_2$ , petroleum ether/ethyl acetate, gradient: 0% → 60%). The product was obtained as a colorless solid (580 mg, 50%). Analyses were in accordance with the previously published literature [29].

### 2.3. $^1\text{H}$ NMR titration measurements

A solution of **1** was prepared in the appropriate deuterated solvent ( $2.0 \cdot 10^{-3}$  M) and 1.0 mL was pipetted in a NMR tube. The sample was referenced to the residual solvent signal. Then, the complexation of cations with **1** was studied. A 0.1 M solution of the metal perchlorate was prepared in the same solvent. Next, stepwise portions (2  $\mu\text{L}$ ) of the respective perchlorate solution were added into the NMR tube containing the ligand, and after extensive mixing the complexation-induced shifts were recorded. At a ligand:metal ratio of 2:3, 30  $\mu\text{L}$  portions of a 1.0 M perchlorate salt solution were used, and stepwise additions were continued until a ligand:metal ratio of 1:6 was reached to exclude the formation of a complex with another stoichiometry. The displacements of selected  $^1\text{H}$  NMR signals of ligand **1** upon addition of the perchlorate salt were used to calculate the complex stability constants. The calculations were performed using the WinEQNMR2 software [42]. The advised range for the data input covers the addition of metal to ligand from 0.1 to 0.9 equivalents. This instruction was followed and 9 points in this range were measured (steps of 0.1 equiv.) and used for the calculation. The formation of a 1:1 complex was proven by plotting the changes of selected signals against the cation to chelate ratio, observing the change of the slope at a ligand:metal ratio of 1:1.

### 2.4. $^{207}\text{Pb}$ NMR titration measurements

A solution of lead (II) perchlorate trihydrate in acetonitrile- $d_3$  ( $5.0 \cdot 10^{-2}$  M) and a solution of ligand **1** in acetonitrile- $d_3$  ( $1.0 \cdot 10^{-1}$  M) were prepared. A 1.0 mL aliquot of the lead solution was pipetted in a NMR tube. The sample was measured and the  $^{207}\text{Pb}$  signal determined. Next, stepwise portions of ligand **1** (40  $\mu\text{L}$ , 0.08 equiv.) were added into the NMR tube containing the lead solution, and the spectra were recorded after extensive mixing.

## 3. Results and Discussion

### 3.1. Initial $^1\text{H}$ NMR Studies

To determine the stability constant for the complexation of  $\text{Ba}^{2+}$ ,  $\text{Sr}^{2+}$ , and  $\text{Pb}^{2+}$ , a reliable method was developed using  $^1\text{H}$  NMR spectroscopy. To study the influence of the solvent on the complexation and to optimize shift characterization, NMR measurements involving ligand **1** were carried out in various solvents:  $\text{CDCl}_3$ ,  $\text{DMSO}-d_6$ , acetone- $d_6$ , acetonitrile- $d_3$ , and methanol- $d_4$ . Since ligand **1** is not soluble in aqueous solutions,  $\text{D}_2\text{O}$  was not used. Afterward, stability constant measurements were performed using  $\text{Ba}^{2+}$ ,  $\text{Sr}^{2+}$ ,  $\text{Pb}^{2+}$ ,  $\text{Na}^+$ , and  $\text{Bu}_4\text{N}^+$  as their perchlorate salts in acetonitrile- $d_3$ .

First, the protons of ligand **1** were assigned to their signals. The  $^1\text{H}$  NMR spectra of **1** in different solvents are shown in Fig. 1 and the assignment with the chemical shifts is listed in Table 1. A  $\text{C}_2$ -symmetry is found for ligand **1** which results in the number of 12  $^1\text{H}$  signals.

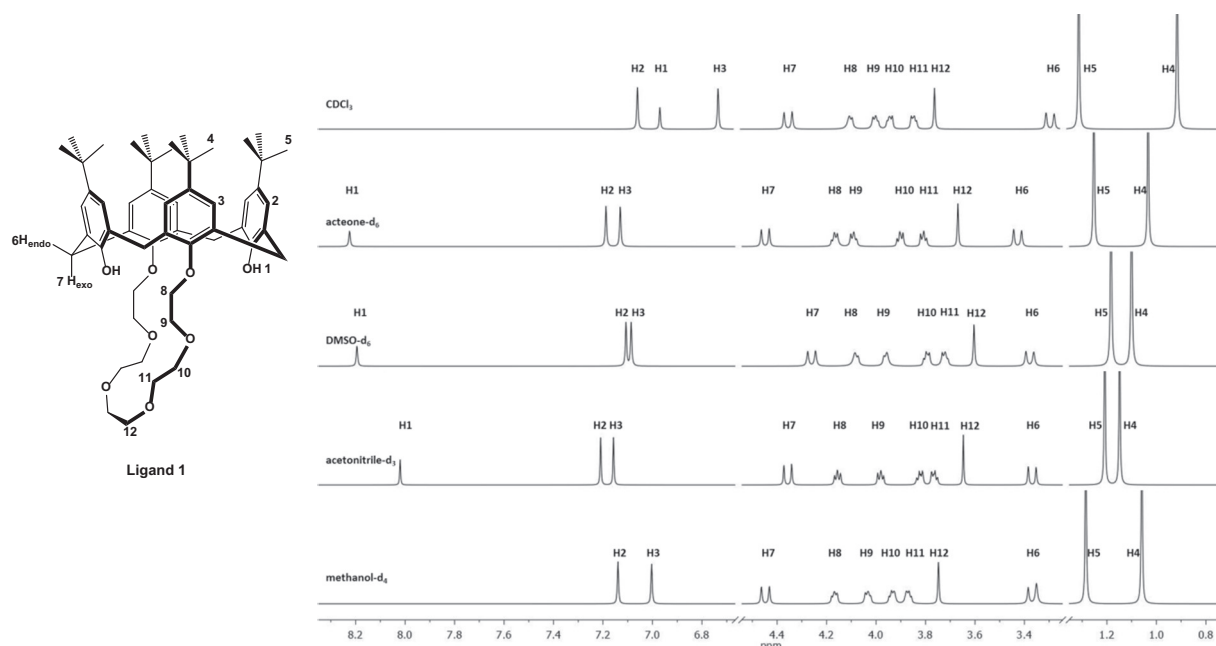


Fig. 1.  $^1\text{H}$  NMR spectra of ligand **1** in different solvents (solvent peaks have been removed for clarity).

Next, the titration method had to be developed, which was representatively executed with  $\text{Ba}^{2+}$  as guest ion. For the calculation of stability constants, the chemical shifts had to be exactly determined [43]. To ensure this, the changes of the chemical shifts in the  $^1\text{H}$  signals between ligand **1** and the  $\text{Ba}^{2+}$  complex must be sufficiently pronounced. For this reason, it had to be ascertained which solvent is most advantageous [44]. Since the solubility of the perchlorate salts is very low in  $\text{CDCl}_3$  and the solubility of the formed complexes is also insufficient, this solvent could not be used. Remarkably, upon addition of barium perchlorate to a solution of **1** in  $\text{DMSO}-d_6$  there was no change visual in the  $^1\text{H}$  spectra. This can be attributed to the formation of Ba-DMSO-complexes which are described in the literature [45]. Once formed, these complexes are not interacting with the calix[4]crown anymore. The DMSO-interaction is discussed in more detail later. The use of acetone- $d_6$  and methanol- $d_4$  showed clear changes in the spectra comparing the ligand and the 1:1 complex. However, the strongest difference was obtained in acetonitrile- $d_3$  which makes it the favorable solvent for the titration experiment (see SI for spectra).

Consequently, all NMR titration experiments were performed in acetonitrile- $d_3$ . Therefore,  $^1\text{H}$  NMR spectra of a  $2.0 \cdot 10^{-3}$  M solution (1 mL) of **1** were measured upon stepwise addition (2  $\mu\text{L}$ ) of a 0.1 M solution of the perchlorate (prepared in acetonitrile- $d_3$ ). Each step represents the addition of 0.1 equiv. of the metal perchlorate to ligand **1**. In Fig. 2, the titration experiment with  $\text{Ba}^{2+}$  is shown. Shifts for all proton signals are observed.

The differences of the chemical shifts  $\Delta\delta_{\text{H2-H3}}$ ,  $\Delta\delta_{\text{H7-H6}}$  and  $\Delta\delta_{\text{H5-H4}}$  upon  $\text{Ba}^{2+}$  addition indicate a significant alteration in the orientation of the aromatic rings.  $\Delta\delta_{\text{H7-H6}}$  decreased from 0.99 ppm (ligand) to 0.47 ppm (1:1 complex). The shifting of these doublets is related to a twisting of the aromatic rings [46]. The general presence of the doublets proves the fixed cone conformation, since a free rotation of the aryl rings would cause only a singlet [47]. The distance between the doublets H6 and H7 results from the orientation of the protons into or out of the aromatic ring current and gives information about the cone flattening [48]. The difference in the chemical shift between the axial (H7) and equatorial (H6) protons ( $\Delta\delta_{\text{H7-H6}}$ ) gets smaller when the aromatic rings rotate (Fig. 3). It can be deduced from Fig. 2 that the two non-

Table 1  
 $^1\text{H}$  NMR (400 MHz,) shifts of compound **1**.

$^1\text{H}$ Signal <sup>a</sup>	Multiplicity [Hz]	Integral	Shift [ppm]					Assignment
			$\text{CDCl}_3$	Acetone- $d_6$	$\text{DMSO}-d_6$	Acetonitrile- $d_3$	Methanol- $d_4$	
H1	s	2	6.96	8.22	8.19	8.02	–	OH
H2	s	4	7.07	7.19	7.11	7.21	7.14	Ar-H
H3	s	4	6.74	7.13j	7.09	7.16	7.00	Ar-H
H4	s	18	0.91	1.03	1.10	1.15	1.06	$^t\text{Bu}$
H5	s	18	1.31	1.25	1.18	1.21	1.29	$^t\text{Bu}$
H6	d	4	3.30	3.43	3.38	3.37	3.37	$\text{H}_{\text{endo}}$
H7	d	4	4.36	4.45	4.26	4.36	4.45	$\text{H}_{\text{exo}}$
H8	m	4	4.12–4.08	4.19–4.15	4.10–4.06	4.17–4.14	4.19–4.15	$\text{CH}_2\text{O}$
H9	m	4	4.02–3.98	4.11–4.07	3.98–3.94	4.00–3.96	4.05–4.01	$\text{CH}_2\text{O}$
H10	m	4	3.95–3.92	3.92–3.88	3.81–3.77	3.84–3.81	3.96–3.91	$\text{CH}_2\text{O}$
H11	m	4	3.86–3.82	3.82–3.79	3.74–3.70	3.78–3.75	3.89–3.84	$\text{CH}_2\text{O}$
H12	s	4	3.77	3.67	3.60	3.65	3.75	$\text{CH}_2\text{O}$

<sup>a</sup> Is not representing the IUPAC assignment.

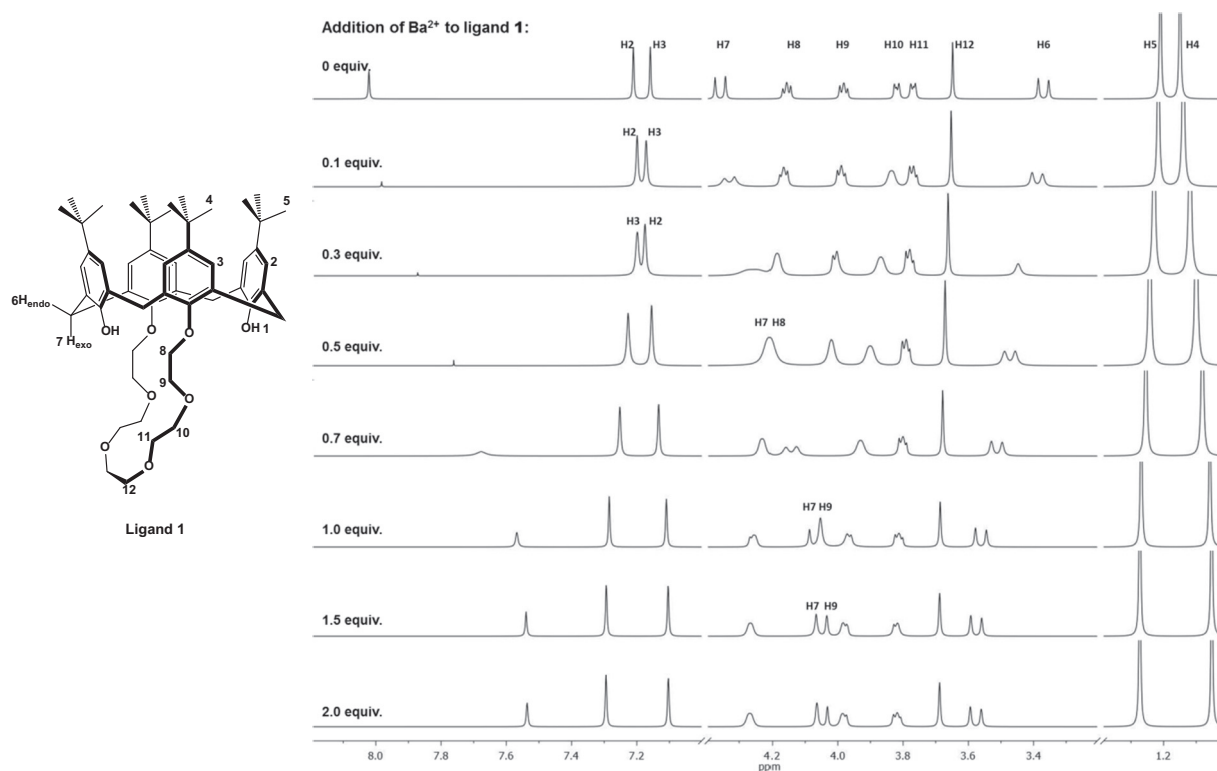


Fig. 2.  $^1\text{H}$  NMR spectra of ligand **1** at different  $\text{Ba}(\text{ClO}_4)_2$  concentrations measured in acetonitrile- $d_3$ .

bridged aromatic rings turn, so that the hydroxyl groups point towards the  $\text{Ba}^{2+}$  ion which is located on the lower rim. This is explained by Fig. 4. When ring B rotates at a certain angle, the *meta*-aryl proton will face ring A frontally. The proton will perceive a lower magnetic field and this will be noticed as a high field shift in NMR measurements. If the proton moves to the outside of ring A, it will perceive a higher magnetic field and this will be noticed as a down field shift. The *tert*-butyl group behaves contrary. When the *meta*-aryl proton of ring B faces ring A, the *tert*-butyl group directs to the outside of ring A and will perceive an increase of the magnetic field strength this results in a displacement of the  $^1\text{H}$  signal to down field. For this reason, H2 and H4 are high field but H3 and H5 down field shifted.

Not only an interaction with the calix cone can be determined but also clear changes in chemical shifts of the crown signals (H8–H12) are observed due to the coordination of  $\text{Ba}^{2+}$  to the ether oxygen atoms. The strongest movements occurred for the chemical shifts of the crown protons H8, H9 and H10, whereas only a slight movement was found for the signals H11 and H12. This indicates that the  $\text{Ba}^{2+}$  is

bound more closely to the lower calix rim, strongly interacting with the aromatic ether oxygen atoms but hardly with the upper ether oxygen atoms of the crown. However, using Fig. 4, another effect can be explained. In the lowest energy conformers of ligand **1** the OH groups form hydrogen bonds with neighboring aromatic ether oxygen atoms and the lower rim is pushed together [11]. As a result of this interaction, the OH signals are located down field ( $\delta = 8.02$  ppm, acetonitrile- $d_3$ ) [49]. The incorporation of the barium ions lead to a conformational change, which is causing a decrease of the hydrogen bonds by opening the lower rim, and therefore a significant shift of the OH groups to the high field is observed ( $\delta = 7.54$  ppm, acetonitrile- $d_3$ ,  $\text{Ba}^{2+}$ -1:1-complex). This is noteworthy, since otherwise, it would be expected that the interaction of barium with the OH groups of ligand **1** would result in a shift to the down field, due to the electron withdrawing effect of the ion.

For evaluation of the data, the four  $^1\text{H}$  signals of H2, H3, H4 and H5 were used since these singlets were easy to follow upon  $\text{Ba}^{2+}$  addition. When the  $^1\text{H}$  shifts are plotted against the equivalents of  $\text{Ba}^{2+}$ , Fig. 5 is

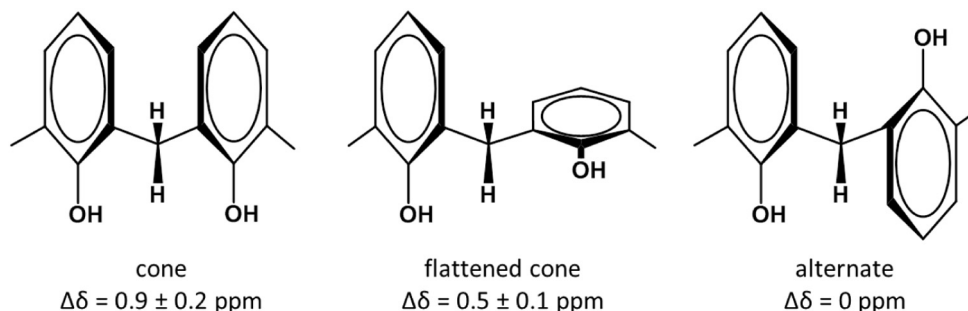


Fig. 3. Conformational dependence of  $\Delta\delta_{\text{H6-H7}}$  [11].



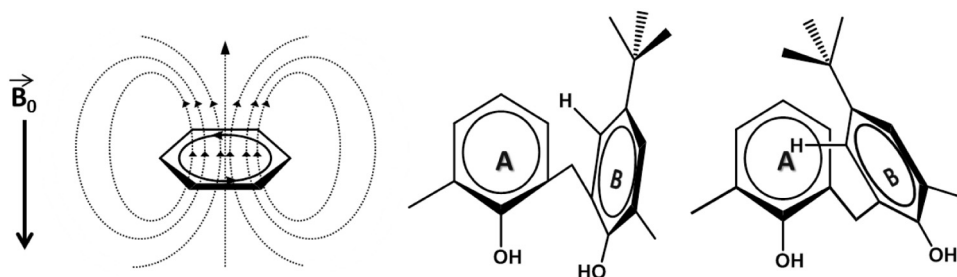


Fig. 4. Conformational dependence of  $\Delta\delta_{\text{H2-H3}}$  and  $\Delta\delta_{\text{H4-H5}}$ .

obtained. All curves show a change of the slope at the ratio of 1:1, indicating the formation of a 1:1 complex.

The same titration method was applied to the perchlorate salts of  $\text{Sr}^{2+}$ ,  $\text{Pb}^{2+}$ ,  $\text{Na}^+$  and  $\text{Bu}_4\text{N}^+$ . For the small  $\text{Na}^+$  and the bulky tetrabutylammonium ion, no changes in the spectra were observed, indicating that **1** shows size selectivity for the cations of interest. Furthermore, these two experiments prove that there is no interaction between the perchlorate and ligand **1**. For the divalent metals  $\text{Sr}^{2+}$  and  $\text{Pb}^{2+}$  incorporation into the calix[4]arene-crown cavity was observed as well, and the formation of a 1:1 complexes was confirmed (see SI).

After the  $^1\text{H}$  NMR shifts upon  $\text{Ba}^{2+}$ ,  $\text{Sr}^{2+}$  and  $\text{Pb}^{2+}$  addition were measured, the stability constants were calculated [42]. The logK values for the 1:1 complex of ligand **1** with  $\text{Ba}^{2+}$ ,  $\text{Sr}^{2+}$  and  $\text{Pb}^{2+}$  calculated for different  $^1\text{H}$  signals are listed in Table 2.

For the calculation of the stability constant of the  $\text{Pb}^{2+}$ -**1** complex, the signal H2 did not move significantly enough and signal H3 was too broad to be used. The calculation was performed with the chemical shifts of signals H4 and H5 only, but due to the shape of these signals with high inaccuracy.

Stability constants for all three metal ions were calculated, whereupon the choice of a specific  $^1\text{H}$  signal plays no significant role for the result. Overall, the highest stability constant was calculated for  $\text{Ba}^{2+}$  (approx. 4.7) followed by  $\text{Sr}^{2+}$  (approx. 4.3) and  $\text{Pb}^{2+}$  (approx. 3.3).

As mentioned before,  $\text{Ba}^{2+}$  appears to be located close to the lower rim of the calix, strongly interacting with the aromatic ether oxygens and barely with the top of the crown. Upon complexation, the  $^1\text{H}$  signals for the hydroxyl protons H1 are high field shifted (Fig. 2). This is not

caused by the ring current effect, but by the diminishing of the hydrogen bonds between the hydroxyl groups and the aromatic ether oxygens.

In contrast,  $\text{Sr}^{2+}$  shows a different interaction with **1**. It can be looked up in the titration experiment data (SI) that the  $^1\text{H}$  signal H2, which shifts strongly for  $\text{Ba}^{2+}$  (Fig. 2), only shifts slightly upon  $\text{Sr}^{2+}$  addition.  $\Delta\delta$ 's listed in Table 3 reveal that the  $\text{Sr}^{2+}$ -**1** complex is not comparably pinched to the  $\text{Ba}^{2+}$ -**1** complex. The H2 signal refers to the *meta*-protons of the non-bridged aromatic rings. This indicates that  $\text{Sr}^{2+}$  is not situated directly at the lower rim of the calix cone, and not actively influencing the orientation of the aromatic rings, like  $\text{Ba}^{2+}$  is. Additionally, there only is a small shift of the OH signals to the high field compared to barium ( $\delta = 7.86$  ppm,  $\text{Sr}^{2+}$ -1:1-complex /  $\delta = 7.54$  ppm,  $\text{Ba}^{2+}$ -1:1-complex), showing, that there is only a minor opening of the lower rim. It is supposed to sit lower in the crown and the wrapping of the crown around  $\text{Sr}^{2+}$  leads to a pinch of exclusively the two attached aromatic rings. As a result, the *meta*-aryl protons referring to the H3 signal are facing the other two aromatic rings which is confirmed by the down field shift of signal H3. The rotation of the rings can be confirmed by the  $\Delta\delta_{\text{H7-H6}}$  value. Other than barium, strontium induces significant shifts for the  $^1\text{H}$  crown signals H11 and H12, proving that it is situated in the lower crown. These facts confirm a different binding mode. The reason why  $\text{Sr}^{2+}$  is not incorporated into the calix cone might be the significant smaller ionic radius. For a similar interaction as  $\text{Ba}^{2+}$ ,  $\text{Sr}^{2+}$  would demand a greater pinch of the cone. Considering the necessary tension of the cone, it is comprehensible that interaction of the strontium and the aromatic ether oxygens is not advantageous. This is resulting in a stronger interaction with the ether oxygens in the middle of the crown. It is notable that only the smaller radius, considering similar chemical properties of both ions, results in a decrease of the stability constant. Since the radius of  $\text{Ra}^{2+}$  is slightly bigger than the radius of  $\text{Ba}^{2+}$  it might result in a small increase of the complex stability.

$\text{Pb}^{2+}$  has a similar size to  $\text{Sr}^{2+}$ , but different chemical properties. Upon addition of lead perchlorate to ligand **1** the proton signals of the measured spectra appeared very broad and almost vanished (for titration experiment data see SI). Interestingly,  $^1\text{H}$  signal H2 was the only one, which was barely affected upon the titration, like it is for  $\text{Sr}^{2+}$ . As soon as reaching the 1:1 ratio, the signals are again sharply defined. This behavior indicates a fast exchange of  $\text{Pb}^{2+}$  between the free ligands and the complex during the timescale of a  $^1\text{H}$  measurement. The

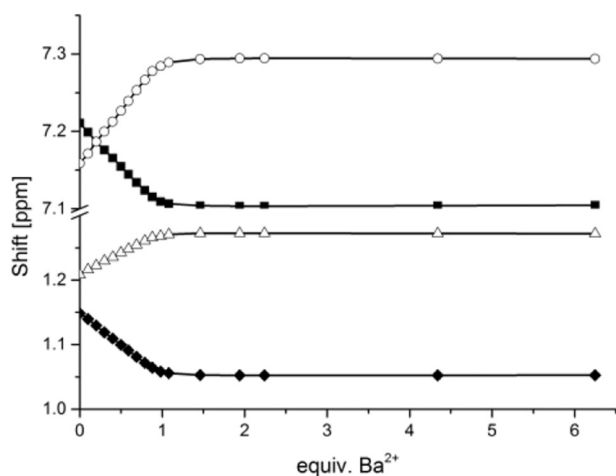


Fig. 5. Shifts of four selected  $^1\text{H}$  NMR signals of **1** at different  $\text{Ba}(\text{ClO}_4)_2$  concentrations measured in acetonitrile- $d_3$ . ○: shift of H2, ■: shift of H3, △: shift of H5, ◆: shift of H4.

Table 2  
Stability constants for ligand **1** determined by  $^1\text{H}$  NMR titration experiment in acetonitrile- $d_3$ .

Cation	Stability constants, determined by selected $^1\text{H}$ signals			
	H2	H3	H4	H5
$\text{Ba}^{2+}$	$4.6 \pm 0.1$	$4.9 \pm 0.2$	$4.6 \pm 0.1$	$4.8 \pm 0.2$
$\text{Sr}^{2+}$	–	$4.4 \pm 0.1$	$4.3 \pm 0.1$	$4.3 \pm 0.2$
$\text{Pb}^{2+}$	–	–	$3.3 \pm 1$	$3.2 \pm 1$

**Table 3**

Comparison of the  $\Delta\delta$  of ligand **1** and its 1:1 complexes (negative values represent the crossing of the two peaks).

Compound	$\Delta\delta_{\text{H2-H3}}$	$\Delta\delta_{\text{H7-H6}}$	$\Delta\delta_{\text{H5-H4}}$
Ligand <b>1</b>	0.05	0.99	0.06
Ba <sup>2+</sup> -1:1 Complex	−0.19	0.47	0.22
Sr <sup>2+</sup> -1:1 Complex	−0.11	0.43	0.15
Pb <sup>2+</sup> -1:1 Complex	−0.08	0.49	0.14

titration also reveals a strong interaction with the crown, indicating that Pb<sup>2+</sup> is situated only in the crown, and the wrapping of the crown around Pb<sup>2+</sup> leads to the pinch of the cone, comparable to Sr<sup>2+</sup>. Comparing the  $\Delta\delta$ 's in Table 1 the pinch is least distinct for this guest ion. Furthermore, there is no significant shift of the OH signals to the high field, showing intact hydrogen bonds and no opening of the lower rim. Pb<sup>2+</sup> shows a low stability constant in this study, the calix scaffold seems to have no significant effect on this ion.

### 3.2. Pb <sup>207</sup>Pb NMR Studies

Since <sup>207</sup>Pb (natural abundance: 22.6%) has a medium sensitivity NMR spin-1/2 nucleus [50,51], <sup>207</sup>Pb NMR is a valuable and helpful tool to describe the chemical situation in the Pb-calix complex. Thus, <sup>207</sup>Pb spectra were recorded upon ligand **1** addition to a 1 M Pb(ClO<sub>4</sub>)<sub>2</sub> solution. In contrast to the <sup>1</sup>H nucleus, the relaxation time for the <sup>207</sup>Pb nucleus is very short. During this short time range no exchange process of the lead ion between ligand **1** and the complex Pb<sup>2+</sup>-**1** was observed. As a result, the received spectra (Fig. 6) show two signals: a decreasing signal for the free Pb<sup>2+</sup> at  $\delta = -3380$  ppm and an increasing signal for the Pb-calix-complex downfield shifted at  $\delta = -3100$  ppm. A slight shift for the free Pb<sup>2+</sup> signal is noticed and is dependent on the free metal ion

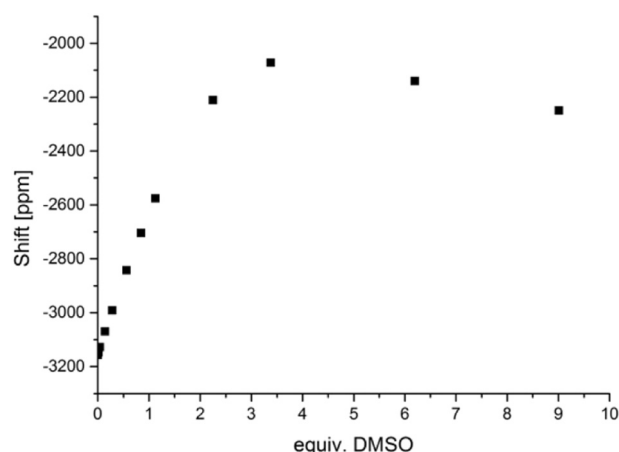


**Fig. 7.** Shift of the <sup>207</sup>Pb NMR signal upon DMSO addition to a 1 M Pb(ClO<sub>4</sub>)<sub>2</sub> solution in acetonitrile-*d*<sub>3</sub>.

concentration (see SI and [52]). This data confirms the formation of a 1:1 complex, but it cannot be used for the calculation of the stability constant.

To confirm the previously mentioned complexation of Pb<sup>2+</sup> with DMSO, an additional experiment was examined. The <sup>207</sup>Pb NMR titration was repeated with stepwise addition of DMSO to a 1 M Pb(ClO<sub>4</sub>)<sub>2</sub> solution instead of ligand **1** (Fig. 7, see also SI). A strong shift of the Pb<sup>2+</sup> signal upon DMSO addition was observed. This proves the formation of Pb<sup>2+</sup>-DMSO complexes which are also expected for barium and strontium [45]. This fact makes it impossible to perform the titration experiments in DMSO-*d*<sub>6</sub>, as discussed previously.

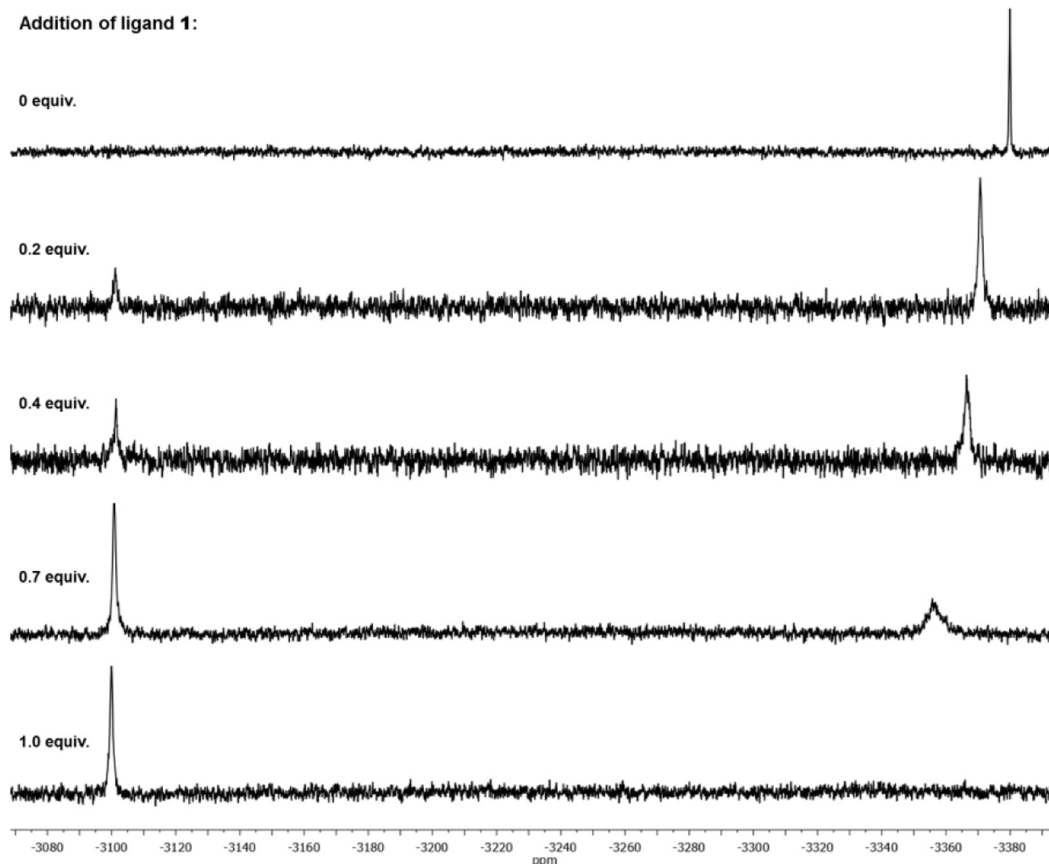


**Fig. 6.** <sup>207</sup>Pb NMR spectra at different ligand concentrations measured in acetonitrile-*d*<sub>3</sub>.

## 4. Conclusion

Titration experiments of  $\text{Ba}^{2+}$ ,  $\text{Sr}^{2+}$  and  $\text{Pb}^{2+}$  with ligand **1** were successfully performed and the stability constants were determined by NMR measurements in acetonitrile- $d_3$ . Insights were derived from the data obtained, whereby structure-interaction-relationships of the complexes could be revealed. Compound **1** shows promising properties for  $\text{Ba}^{2+}$  which is not only a metal of radiopharmaceutical interest, but, also serves in this study as a surrogate for  $\text{Ra}^{2+}$ . For this reason further investigations with radium and calixcrowns are planned. However,  $\text{Sr}^{2+}$  does not have the same binding mode, most likely due to its smaller ionic radius. Strontium resembles the behavior of lead, and appears to interact exclusively with the ether crown moiety of **1**. Since the homologous radium has only a slightly larger radius than barium, it can be assumed that the synergetic effect of **1** is similar for both metals. Several modifications are in progress to increase the stability constants to an appropriate level for radiopharmaceutical applications. The two free hydroxyl groups offer the possibility of additional functions to increase the stability for heavy group 2 metals.

## Appendix A. Supplementary data

Supplementary data to this article can be found online at <https://doi.org/10.1016/j.saa.2018.03.029>.

## References

- [1] J. Magill, G. Pfennig, J. Galy, *Karlsruher Nuklidkarte*, 7<sup>th</sup> ed. Haberbeck GmbH, Lage (Germany), 2006.
- [2] H.W. Kirby, M.L. Salutsky, *Radiochemistry of Radium*, Clearinghouse for Federal Scientific and Technical Information (U.S.), 1964.
- [3] M. Gott, J. Steinbach, C. Mamat, *The radiochemical and radiopharmaceutical applications of radium*, *Open Chem.* 14 (2016) 118–129.
- [4] E.J. Hall, A.J. Giaccia, *Radiobiology for the Radiologist*, 6<sup>th</sup> ed. Lippincott Williams & Wilkins, Philadelphia, 2006.
- [5] K.D. Mjos, C. Orvig, *Metallodrugs in medicinal inorganic chemistry*, *Chem. Rev.* 114 (2014) 4540–4563.
- [6] R.P. Spencer, R.C. Lange, S. Treves, *Use of Ba-135m and Ba-131 as bone-scanning agents*, *J. Nucl. Med.* 12 (1971) 216–227.
- [7] A. Sonzogni, *Interactive Chart of Nuclides*, <http://www.nndc.bnl.gov/chart/> (accessed: 30.10.2017).
- [8] F. Hosain, I.B. Syed, H.N. Wagner Jr., J.K. Poggenburg, *Ionic barium 135 m: a new agent for bone scanning*, *Radiology* 98 (1971) 684–686.
- [9] J.H. Kearsley, R.S. Fitchew, R.G. Taylor, *Adjunctive radiotherapy with strontium-90 in the treatment of conjunctival squamous cell carcinoma*, *Int. J. Radiat. Oncol. Biol. Phys.* 14 (1988) 435–443.
- [10] S. Laskar, L. Gurram, S.G. Laskar, S. Chaudhari, N. Khanna, R. Upreti, *Superficial ocular malignancies treated with strontium-90 brachytherapy: long term outcomes*, *J. Contemp. Brachyther.* 7 (2015) 369–373.
- [11] C.D. Gutsche, *Calixarenes: An Introduction*, 2<sup>nd</sup> ed. The Royal Society of Chemistry, 2008.
- [12] G. McMahon, S. O'Malley, K. Nolan, D. Diamond, *Important calixarene derivatives - their synthesis and applications*, *ARKIVOC* (2003) 23–31.
- [13] M. Deska, B. Dondela, W. Sliwa, *Selected applications of calixarene derivatives*, *ARKIVOC* (2015) 393–416.
- [14] W. Sliwa, C. Kozłowski, *Calixarenes and Resorcinarenes*, Wiley-VCH, Germany, Weinheim, 2009.
- [15] M. Mourer, R.E. Duval, C. Finance, J.B. Regnouf-de-Vains, *Functional organisation and gain of activity: the case of the antibacterial tetra-para-guanidinoethyl-calix[4]arene*, *Bioorg. Med. Chem. Lett.* 16 (2006) 2960–2963.
- [16] R.B. Shah, N.N. Valand, P.G. Sutariya, S.K. Menon, *Design, synthesis and characterization of quinoline-pyrimidine linked calix[4]arene scaffolds as anti-malarial agents*, *J. Incl. Phenom. Macrocycl. Chem.* 84 (2016) 173–178.
- [17] E. Da Silva, A.N. Lazar, A.W. Coleman, *Biopharmaceutical applications of calixarenes*, *J. Drug Delivery Sci. Technol.* 14 (2004) 3–20.
- [18] A. Yousaf, S.A. Hamid, N.M. Bunnori, A.A. Ishola, *Applications of calixarenes in cancer chemotherapy: facts and perspectives*, *Drug Des. Devel. Ther.* 9 (2015) 2831–2838.
- [19] A.I. Vovk, L.A. Kononets, V.Y. Tanchuk, S.O. Cherenok, A.B. Drapailo, V.I. Kalchenko, V.P. Kukhar, *Inhibition of Yersinia protein tyrosine phosphatase by phosphonate derivatives of calixarenes*, *Bioorg. Med. Chem. Lett.* 20 (2010) 483–487.
- [20] G. Arena, A. Casnati, A. Contino, A. Magri, F. Sansone, D. Sciotto, R. Ungaro, *Inclusion of naturally occurring amino acids in water soluble calix[4]arenes: a microcalorimetric and 1H NMR investigation supported by molecular modeling*, *Org. Biomol. Chem.* 4 (2006) 243–249.
- [21] A. Depauw, N. Kumar, M.H. Ha-Thi, I. Leray, *Calixarene-based fluorescent sensors for cesium cations containing BODIPY fluorophore*, *J. Phys. Chem. A* 119 (2015) 6065–6073.
- [22] A.L. Maksimov, T.S. Buchneva, E.A. Karakhanov, *Supramolecular calixarene-based catalytic systems in the Wacker-oxidation of higher alkenes*, *J. Mol. Catal. A Chem.* 217 (2004) 59–67.
- [23] B.B. Adhikari, M. Kanemitsu, H. Kawakita, K. Ohto Jumina, *Synthesis and application of a highly efficient polyvinylcalix[4]arene tetraacetic acid resin for adsorptive removal of lead from aqueous solutions*, *Chem. Eng. J.* 172 (2011) 341–353.
- [24] S. Kunsagi-Mate, K. Szabo, B. Desbat, J.L. Brunel, I. Bitter, L. Kollar, *Complexation of phenols by calix[4]arene Diethers in a low-permittivity solvent. Self-switched complexation by 25,27-Dibenzoyloxycalix[4]arene*, *J. Phys. Chem. B* 111 (2007) 7218–7223.
- [25] G. Henriksen, P. Hoff, R.H. Larsen, *Evaluation of potential chelating agents for radium*, *Appl. Radiat. Isot.* 56 (2002) 667–671.
- [26] G.J. Lumetta, R.D. Rogers, A.S. Gopalan, *Calixarenes for Separations*, American Chemical Society, Washington, DC, 2000.
- [27] C. Alfieri, E. Dradi, A. Pochini, R. Ungaro, G.D. Andreotti, *Synthesis, and X-ray crystal and molecular-structure of a novel macrobicyclic ligand - crowned para-tert-butyl-calix[4]arene*, *J. Chem. Soc. Chem. Commun.* (1983) 1075–1077.
- [28] J.S. Kim, W.K. Lee, W. Sim, J.W. Ko, M.H. Cho, D.Y. Ra, J.W. Kim, *Calix[4]arenes bridged with two different crown ether loops: influence of crown size on metal ion recognition*, *J. Incl. Phenom. Macrocycl. Chem.* 37 (2000) 359–370.
- [29] H. Zhou, K. Surowiec, D.W. Purkiss, R.A. Bartsch, *Proton di-ionizable p-tert-butylcalix[4]arene-crown-6 compounds in cone, partial-cone and 1,3-alternate conformations: synthesis and alkaline earth metal cation extraction*, *Org. Biomol. Chem.* 3 (2005) 1676–1684.
- [30] H. Zhou, D. Liu, J. Gega, K. Surowiec, D.W. Purkiss, R.A. Bartsch, *Effect of para-substituents on alkaline earth metal ion extraction by proton di-ionizable calix[4]arene-crown-6 ligands in cone, partial-cone and 1,3-alternate conformations*, *Org. Biomol. Chem.* 5 (2007) 324–332.
- [31] A.L. Boston, E.K. Lee, K. Surowiec, J. Gega, R.A. Bartsch, *Comparison of upper and lower rim-functionalized, di-ionizable calix[4]arene-crown-6 structural isomers in divalent metal ion extraction*, *Tetrahedron* 68 (2012) 8789–8794.
- [32] A.F. Holleman, E. Wiberg, N. Wiberg, *Lehrbuch der anorganischen Chemie*, De Gruyter, Berlin, 2007.
- [33] F.W. van Leeuwen, W. Verboom, D.N. Reinhoudt, *Selective extraction of naturally occurring radioactive  $\text{Ra}^{2+}$* , *Chem. Soc. Rev.* 34 (2005) 753–761.
- [34] F.W. van Leeuwen, H. Beijleveld, A.H. Velders, J. Huskens, W. Verboom, D.N. Reinhoudt, *Thiacalix[4]arene derivatives as radium ionophores: a study on the requirements for  $\text{Ra}^{2+}$  extraction*, *Org. Biomol. Chem.* 3 (2005) 1993–2001.
- [35] F.W.B. van Leeuwen, H. Beijleveld, C.J.H. Miermans, J. Huskens, W. Verboom, D.N. Reinhoudt, *Ionizable (Thia)calix[4]crowns as Highly Selective  $^{226}\text{Ra}^{2+}$  Ionophores*, *Anal. Chem.* 77 (2005) 4611–4617.
- [36] X.Y. Chen, M. Ji, D.R. Fisher, C.M. Wai, *Ionizable calixarene-crown ethers with high selectivity for radium over light alkaline earth metal ions*, *Inorg. Chem.* 38 (1999) 5449–5457.
- [37] G.E. Harrison, T.E.F. Carr, A. Sutton, *Distribution of radioactive calcium strontium barium and radium following intravenous injection into a healthy man*, *Int. J. Radiat. Biol.* 13 (1967) 235–242.
- [38] L. Gmelin, *Gmelins Handbuch der anorganischen Chemie*, Radium, Springer, Berlin, 1977.
- [39] J. Behrends, J. Bischofberger, R. Deutzmann, *Duale Reihe Physiologie*, Georg Thieme Verlag, 2017.
- [40] K. Yong, M. Brechbiel, *Application of  $^{212}\text{Pb}$  for targeted alpha-particle therapy (TAT): pre-clinical and mechanistic understanding through to clinical translation*, *AIMS Med. Sci.* 2 (2015) 228–245.
- [41] K. Yong, M.W. Brechbiel, *Towards translation of  $^{212}\text{Pb}$  as a clinical therapeutic: getting the lead in*, *Dalton Trans.* 40 (2011) 6068–6076.
- [42] M.J. Hynes, *Egnmr - a computer-program for the calculation of stability-constants from nuclear-magnetic-resonance chemical-shift data*, *J. Chem. Soc. Dalton Trans.* (1993) 311–312.
- [43] J.A. Weil, B.C. Wong, J. Yu, *Cautionary note: linewidth effect in dynamic NMR*, *Spectrochim. Acta A Mol. Biomol. Spectrosc.* 77 (2010) 661–664.
- [44] O.V. Surov, M.A. Krestianinov, M.I. Voronova, *Complexation of solvents and conformational equilibria in solutions of the simplest calix[4]arenes*, *Spectrochim. Acta A Mol. Biomol. Spectrosc.* 134 (2015) 121–126.
- [45] J.M. Harrowfield, W.R. Richmond, B.W. Skelton, A.H. White, *Solid-state models of ion solvation: crystal structures of dimethyl sulfoxide solvates of alkaline earth cations*, *Eur. J. Inorg. Chem.* (2004) 227–230.
- [46] A. Arduini, A. Pochini, S. Reverberi, R. Ungaro, *Para-tert-butyl-calix[4]arene tetracarboxylic acid - a water-soluble calixarene in a cone structure*, *J. Chem. Soc. Chem. Commun.* (1984) 981–982.
- [47] H. Kammerer, G. Happel, F. Caesar, *Spectroscopic analysis of a cyclic tetrameric compound prepared from p-cresol and formaldehyde*, *Makromol. Chem.* 162 (1972) 179–197.
- [48] S. Kanamathareddy, C.D. Gutsche, *Calixarenes - selective functionalization and bridge building*, *J. Organomet. Chem.* 60 (1995) 6070–6075.
- [49] D.M. Rudkevich, *Intramolecular hydrogen bonding in calixarenes*, *Chem. Eur. J.* 6 (2000) 2679–2686.
- [50] J. Mason, *Multinuclear NMR*, Plenum Press, New York, 1987 305–328.
- [51] B. Wrackmeyer, *Application of  $^{207}\text{Pb}$  NMR parameters*, *Annual Reports on NMR Spectroscopy*, Academic Press 2002, pp. 1–37.
- [52] P.G. Harrison, M.A. Healy, A.T. Steel, *Lead-207 chemical shift data for bivalent lead compounds: thermodynamics of the equilibrium  $\text{Pb}(\text{O}_2\text{CCH}_3)_2 \rightleftharpoons [\text{Pb}(\text{O}_2\text{CCH}_3)]^+ + \text{O}_2\text{CCH}_3$  in aqueous solution in the temperature range 303–323 K*, *J. Chem. Soc. Dalton Trans.* (1983) 1845–1848.